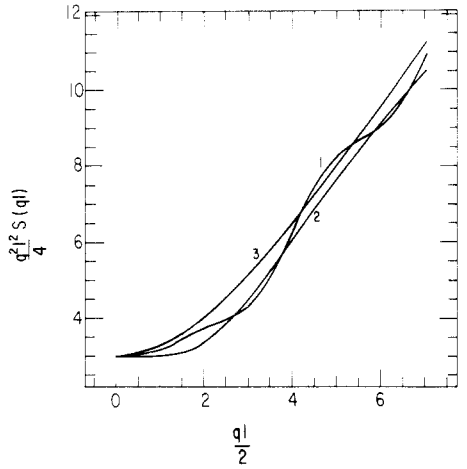

Figure 1. Variation of $(q^2l^2/4)/S(q)$ vs. $ql/2$ for an infinite semiflexible chain as given (1) by the sliding rod model, (2) by Koyama, and (3) by des Cloizeaux.

Gaussian coil discontinuously. When the hydrodynamic interaction is preaveraged

$$F(q) = \frac{1}{3\pi ql}\left[1 - \frac{\sin(ql)}{ql} + \mathrm{Ci}(ql) - \mathrm{Ci}(qd) - \frac{\mathrm{Si}(ql)}{qL}\right] + \frac{2}{\pi\pi^{1/2}q^2l^2}\left[\gamma\left(\frac{3}{2},\frac{q^2Ll}{6}\right) - \gamma\left(\frac{1}{2},\frac{q^2l^2}{6}\right)\right] - \frac{12}{\pi\pi^{1/2}q^4Ll^3}\left[\gamma\left(\frac{3}{2},\frac{q^2Ll}{6}\right) - \gamma\left(\frac{3}{2},\frac{q^2l^2}{6}\right)\right] \quad (9)$$

In these expressions, the sine integral, cosine integral, and the incomplete γ function have been used:

$$\mathrm{Si}(x) = \int_0^x \mathrm{d}t\,\frac{\sin t}{t}; \qquad \mathrm{Ci}(x) = -\int_x^\infty \mathrm{d}t\,\frac{\cos t}{t}$$

$$\gamma(m,x) = \int_0^x \mathrm{d}t\; e^{-t}t^{m-1}$$

Also a cutoff hydrodynamic thickness d associated with the chain has been introduced to avoid a singularity in $F(q)$ at zero contour length. The rigid rod limit of the apparent diffusion coefficient $D_{app}(q) = \Gamma(q)/q^2$ is obtained for $l = L$ as

$$D_{app}(q) = \left(D_0 + 2D_0\left[1 - \frac{\sin(qL)}{ql} + \mathrm{Ci}(qL) - \mathrm{Ci}(qd) - \frac{\mathrm{Si}(qL)}{qL}\right]\right)\Big/\left(\frac{2}{qL}\left[\mathrm{Si}(qL) + \frac{\cos(qL) - 1}{qL}\right]\right) \quad (10)$$

where $D_0 = k_BT/\zeta N$. Equations 10 and 4a have the same small qL limit

$$\lim_{q\to 0} D_{app}(q) = D_0 + 2D_0[\ln(L/d) - 1] \quad (11)$$

if both the free-draining and nondraining values are considered to define D as $D = D_0 + 2D_0[\ln(L/d) - 1]$. Note that when the length of the rod becomes large, eq 10 becomes

$$\lim_{qL\to\infty} D_{app}(q) = D_0\frac{qL}{\pi} + 2D_0\left[0.423 + \ln\left(\frac{1}{qd}\right)\right]\frac{qL}{\pi} \quad (12)$$

where the expansion $\lim_{qd\to 0}\mathrm{Ci}(qd) \simeq 0.577 + \ln(qd)$ has been used. Equation 12 is different from eq 5. In eq 12, $D_{app}(q)$ increases linearly with qL for a fixed D whereas in eq 5 it reaches a plateau value at large qL. As pointed out before,[8,9] this discrepancy comes from the fact that eq 6 uses the full configuration space whereas eq 1 includes rigid constrainsts at the outset. For example, eq 6 gives for freely jointed chains[10] the same limit at large q as for flexible chains. We therefore conclude that the sliding rod model, as originally presented, i.e., based on eq 6, is valid for semiflexible chains with a small degree of stiffness, i.e., close to flexible coils.

For nonpreaveraged hydrodynamic interaction, the analysis is more involved but tractable to a point. For simplicity we present the infinitely long chain result only:

$$F(q) = \frac{1}{3\pi ql}\left[1 - \frac{\sin(ql)}{ql} + \mathrm{Ci}(ql) - \mathrm{Ci}(qd)\right] + \frac{2}{3\pi q^3l^3}\left[\frac{\sin(ql)}{ql} - \cos(ql)\right] + \frac{3}{\pi\pi^{1/2}q^2l^2}\int_0^1 \mathrm{d}z\,\frac{z^2}{(1-z^2)^{1/2}}\left[\Gamma\left(\frac{1}{2}\right) - \gamma\left(\frac{1}{2},\frac{q^2l^2}{6}\right)(1-z^2)\right] + \frac{3}{\pi\pi^{1/2}q^2l^2}\left(\frac{6}{q^2l^2}\right)^{1/2}\left[\int_0^1 \mathrm{d}z\; e^{(-q^2l^2/6)(1-z^2)} - 1\right] \quad (13)$$

The remaining integrations over the variable z would have to be performed numerically.

Using this continuous limit of the sliding rod model, Stockmayer and Hammouda have estimated[11] corrections to the first cumulant due to a small degree of stiffness ($l \simeq 20$ Å for polystyrene); these corrections have been found to be small.

Acknowledgment. Enlightening discussions with Professor W. H. Stockmayer are greatly appreciated. This work was supported by the National Science Foundation under Grant No. 79-13227, Division of Materials Research, Polymers Program.

References and Notes

(1) Wilcoxon, J.; Schurr, J. M. *Biopolymers* **1983**, *22*, 849.
(2) Maeda, T.; Fujime, S. *Macromolecules* **1984**, *17*, 1157.
(3) Benmouna, M.; Akcasu, A. Z.; Daoud, M. *Macromolecules* **1980**, *13*, 1703.
(4) Akcasu, A. Z.; Gürol, H. *J. Polym. Sci., Polym. Phys. Ed.* **1976**, *14*, 1.
(5) des Cloizeaux, J. *Macromolecules* **1973**, *6*, 402.
(6) Koyama, R. *J. Phys. Soc. Jpn.* **1973**, *34*, 1029.
(7) Yamakawa, H. "Modern Theory of Polymer Solutions"; Harper and Row: New York, 1971.
(8) Stockmayer, W. H.; Burchard, W. *J. Chem. Phys.* **1979**, *70*, 3138.
(9) Akcasu, A. Z.; Benmouna, M.; Han, C. C. *Polymer* **1980**, *21*, 866.
(10) Akcasu, A. Z.; Higgins, J. S. *J. Polym. Sci., Polym. Phys. Ed.* **1977**, *15*, 1745.
(11) Stockmayer, W. H.; Hammouda, B., to be published.

Dielectric Normal Mode Process in Solutions of Polychloroprene

KEIICHIRO ADACHI* and TADAO KOTAKA

Department of Macromolecular Science, Faculty of Science, Osaka University, Toyonaka, Osaka 560, Japan.
Received May 16, 1984

In our recent papers,[1,2] we reported that bulk *cis*-polyisoprene (*cis*-PI) exhibits dielectric relaxation due to

0024-9297/85/2218-0294$01.50/0 © 1985 American Chemical Society

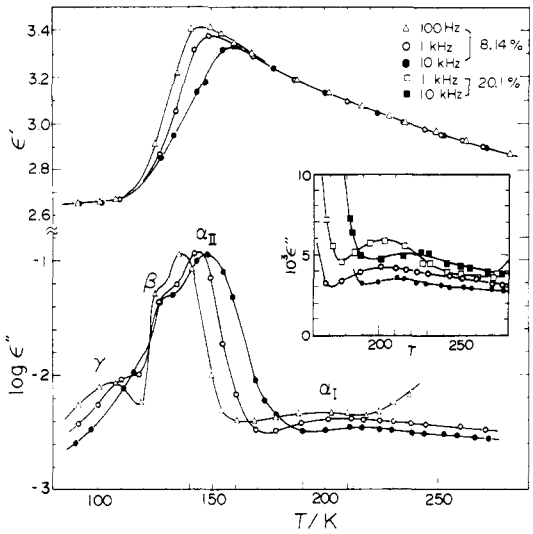

Figure 1. Temperature dependence of ϵ' and log ϵ'' for the 8.14% (by weight) solution of CR(1), and temperature dependence of ϵ'' in the α_I relaxation region for 8.14% and 20.1% solutions of CR(1).

fluctuation of the end-to-end vector, termed the "normal mode process".[3-11] Since the stereochemical structures of polychloroprene (CR) and *cis*-PI are similar, CR should have a component of the dipole moment parallel to the chain contour and exhibit a normal mode process. However, there exists a significant difference in the microstructures between *cis*-PI and CR samples used in this study. Namely, CR contains a large number of head-to-head (h–h) and tail-to-tail (t–t) linkages, where the direction of the moment changes. Such polymers exhibit the normal mode process due to the end-to-end fluctuation of submolecules between the neighboring h–h and t–t linkages but not that of the whole molecule. We may designate the average number of monomer units in the submolecules as the "dipole persistent number". The Rouse–Zimm theory[12,13] predicts that the relaxation time for such motions corresponds to the kth normal mode whose half-wavelength is equal to the length of the submolecule. Baur and Stockmayer[6] reported such relaxation for poly(propylene oxide), in which the parallel dipole changes its direction at the midpoint of the molecule. They found that the relaxation time corresponds to the second normal mode of the whole molecule. In CR, the situation is more complicated, because h–h and t–t linkages occur frequently. From this view, we investigated dielectric properties of toluene solutions of CR to clarify how the microstructure influences the dielectric behavior.

Experimental Section

Two commercial neoprenes, CR(1) and CR(2) (Showa Neoprene Co., Ltd.), were used. They were purified by reprecipitation from benzene into methanol. The precipitates were dried under vacuum of 10^{-1} Pa at room temperature for 1 week. Toluene was distilled with CaH_2. Methods of characterization and the dielectric measurements were described previously.[1,10] The microstructure was analyzed by ^{13}C NMR based on the assignment described by Ebdon.[14] The results of characterization are given in Table I.

Results and Discussion

Figure 1 shows the temperature dependence of the dielectric constant ϵ' and the logarithm of the loss factor ϵ'' for an 8.1 wt % solution of CR(1). The temperature dependence of ϵ'' in the range from 160 to 280 K for 8.14% and 20.1% solutions of CR(1) is also shown in the same figure. Four loss maxima seen in Figure 1 were designated as α_I, α_{II}, β, and γ processes. A similar loss vs. temperature

Table I
Characteristics of Chloroprene Rubber

code	$10^{-4}M_w$	M_w/M_n	microstructure,[a] % h – t trans	h – t cis	h–h and t–t
CR(1)	61	12	73.4	5.5	21.1
CR(2)	3.5	3.5	74.4	5.2	20.4

[a] h–t, h–h, and t–t denote head-to-tail, head-to-head, and tail-to-tail linkages.

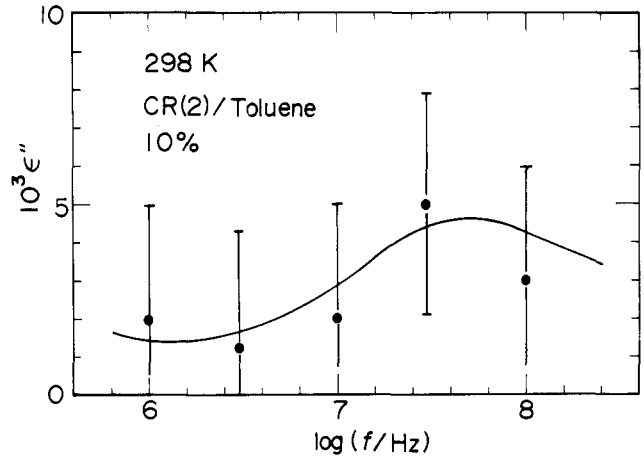

Figure 2. Frequency dependence of ϵ'' at 298 K for a 10% (by weight) solution of CR(2).

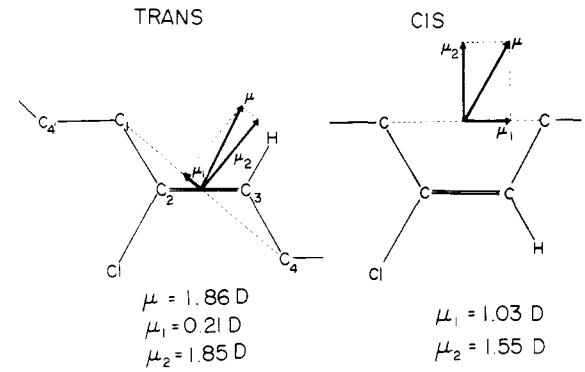

Figure 3. Parallel (μ_1) and perpendicular (μ_2) components of the dipole moment of polychloroprene.

curve was observed for solutions of CR(2). Figure 2 shows the frequency dependence of ϵ'' for a 10 wt % solution of CR(2) at 298 K in the range from 1 to 100 MHz. Though the experimental error was relatively large, a weak loss maximum due to the α_I process was observed in this range. The dielectric relaxation strength $\Delta\epsilon$ for the α_I process was calculated to be 0.015 ± 0.005 from the area of the loss curve.

In Figure 1, the α_{II} process shows the highest loss peak and is attributable to the segmental mode process, because the monomer unit of CR has a strong dipole moment perpendicular to the chain contour besides the parallel component. Since the α_I peak is located at a temperature higher than the temperature range of the α_{II} process due to segmental motions, we assume that the α_I process is due to the normal mode process. In what follows, we discuss the dielectric properties for the α_I process on the basis of this assumption. The features of the α_{II}, β, and γ processes are similar to those in toluene solutions of vinyl polymers[15-18] and will be reported elsewhere.

To check the assignment of the α_I process from $\Delta\epsilon$, we analyzed the dipole moment of CR. Since the dipole

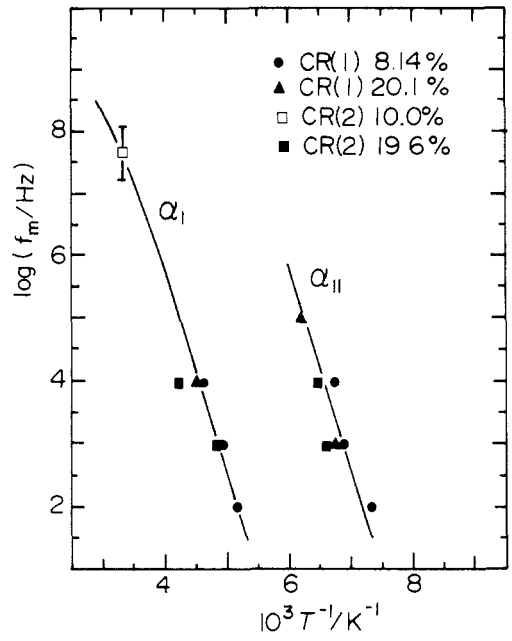

Figure 4. Arrhenius plot for the α_I and α_{II} processes for the solutions of CR(1) and CR(2).

moment of CR arises mostly from the C–Cl bond moment (= 1.86 D),[20] it was decomposed into parallel μ_1 and perpendicular μ_2 components as shown in Figure 3: for the trans unit, μ_1 = 0.21 D and μ_2 = 1.85 D; and for the cis unit, μ_1 = 1.03 D and μ_2 = 1.55 D. Since the C—C=C—C linkage is rigid, we regard the line connecting C_1 and C_4 as a hypothetical bond.[21] It should be noted that μ_1 for the trans unit is much smaller than that for the cis unit, but their directions are opposite.

The theoretical $\Delta\epsilon$ for the normal mode process in a solution with concentration c (in weight/volume) of a polymer having the end-to-end distance $\langle r^2 \rangle$ is given by[5]

$$\Delta\epsilon = 4\pi c\mu^2 N_a \langle r^2 \rangle (\epsilon_s + 2)^2 / 27 M k_B T \qquad (1)$$

where μ is the dipole moment per unit contour length, ϵ_s is the dielectric constant of the solvent, and N_a, M, and $k_B T$ have the usual meanings. We used the value of $\langle r^2 \rangle / M$ in the unperturbed state.[23] When the length of the monomer unit along the chain contour is b, μ is given by μ_1/b. We calculated μ roughly from μ_1 for the trans unit neglecting the contribution of the cis unit. This may be justified for two reasons: the cis units are separated widely, and they have μ_1 directed oppositely to the trans unit. Thus, $\Delta\epsilon$ for the α_I process was calculated to be 0.013. This agrees roughly with the experimental $\Delta\epsilon$ and confirms the above assignment. By using the Onsager equation,[20] we also calculated $\Delta\epsilon$ for the rotation of μ_2 for the 8.14% solution and obtained $\Delta\epsilon$ = 0.90 at 150 K by taking into account the contributions of both the trans and cis units. This value agrees approximately with the increment of ϵ' around 150 K, indicating that the α_{II} process is due to segmental motions.

Arrhenius plots for the α_I and α_{II} processes for solutions of CR(1) and CR(2) are shown in Figure 4. We recognize that the relaxation frequencies f_m for the α_I and α_{II} processes vary in an almost parallel manner as was found for *cis*-PI.[1] This indicates that the origins of the internal friction for both processes are the same. The activation energies for both processes were 60 ± 3 kJ/mol at 1 kHz. Figure 4 shows that despite the large difference in molecular weight between CR(1) and CR(2), the temperatures of the α_I peak for them are nearly the same. This result is at first glance incompatible with the Rouse–Zimm theory, but is quite resonable if the dipole persistent numbers m in CR(1) and CR(2) are the same.

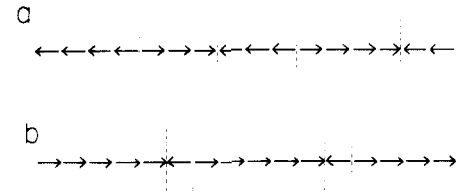

Figure 5. Schematic view of the sequence of the parallel dipole moments.

In the nondraining model, the relaxation time for the kth normal mode τ_k is given by[13]

$$\tau_k = 2[\eta]\eta_0 M / (0.586\lambda_k RT) \qquad (2)$$

where $[\eta]$ is the intrinsic voscosity, η_0 the solvent viscosity, R the gas constant, and λ_k the eigenvalue. For large k, λ_k is given by[22]

$$\lambda_k = (\pi^2 k^{3/2}/2)[1 - (2\pi k)^{-1}] \qquad (3)$$

Though the concentrations of the present CR solutions were in the semidilute range, we used eq 2, which is valid for dilute solutions, because little difference in f_m was observed between 8% and 20% solutions. From $f_m = 4 \times 10^7$ Hz and the data of $[\eta]$ and η_0 at 298 K,[19,23] the value of k was calculated to be 262 and 12.1 for CR(1) and CR(2), respectively. From these values, the molecular weight M_s of the submolecule and the dipole persistent number m were calculated to be 2600 ± 300 and 29 ± 4, respectively.

To discuss the sequence of parallel dipoles, it is necessary to consider the mechanism of the propagation of polymerization. Figure 5 shows a schematic view of the sequence of the parallel dipoles. We assume that polymerization has propagated from the left-hand side to the right-hand side of this figure. For the sake of simplicity, we also assume that all units are linked with trans linkages. If the dipoles pointing to the right (h–t linkage) and those pointing to the left (t–h linkage) exist with the same probability $p/2$, the weight fraction $W(m)$ of the persistent number m is given by $mp^m(1-p)^2$ and the weight average of m (m_w) is equal to $(1+p)/(1-p)$. From the content of h–t linkages given in Table I, m_w was calculated to be 8.5. This value is too small compared with the value of m (m_{obsd}) derived from eq 2.

Next, we assume that whenever an h–h linkage occurs in the polymerization, the next monomer reacts preferentially by the t–t linkage. In this case, the direction of the parallel dipole is inverted immediately after the occurrence of the h–h linkage as shown in Figure 5b so that almost all dipoles are aligned in the same direction. This model b gives M_s comparable with the molecular weight of the whole molecule, which is too large compared with m_{obsd}. It is noted, however, that models a and b in Figure 5 are two extreme cases. If we assume adequate values for the probabilities of the h–t and t–h linkages, we may explain m_{obsd}. However, such a reactivity ratio similar to that in copolymerization kinetics is not yet known.

If we assume the existence of branches with average chain length of 29 monomer units, we can explain the relaxation time for the α_I process. However, to explain $\Delta\epsilon$ by considering branches, we have to assume that CR includes so many branches that more than 50% of the monomer units are incorporated into the branches. At present, there is no evidence to support such a mechanism.

Acknowledgment. This work was supported in part by The Institute of Polymer Research, Osaka University.

References and Notes

(1) Adachi, K.; Kotaka, T. *Macromolecules* **1984**, 17, 120.
(2) Adachi, K.; Kotaka, T. *Macromolecules*, in press.
(3) Stockmayer, W. H. *Pure Appl. Chem.* **1967**, *15*, 539.
(4) North, A. M. *Chem. Soc. Rev.* **1972**, *1*, 49.
(5) Stockmayer, W. H.; Baur, M. E. *J. Am. Chem. Soc.* **1962**, *86*, 3485.
(6) Baur, M. E.; Stockmayer, W. H. *J. Chem. Phys.* **1965**, *43*, 4319.
(7) Stockmayer, W. H.; Burke, J. J. *Macromolecules* **1969**, *2*, 647.
(8) Jones, A. A.; Stockmayer, W. H.; Molinari, R. J. *J. Polym. Sci., Polym. Symp.* **1976**, *54*, 227.
(9) North, A. M.; Phillips, P. J. *Trans. Fraday Soc.* **1968**, *64*, 3235.
(10) Adachi, K.; Kotaka, T. *Macromolecules* **1983**, *16*, 1936.
(11) Hirose, M.; Yamakawa, N.; Araki, K.; Imamura, Y. *Rep. Prog. Polym. Phys. Jpn.* **1977**, *20*, 117.
(12) Rouse, P. E. *J. Chem. Phys.* **1953**, *21*, 1272.
(13) Zimm, B. H. *J. Chem. Phys.* **1956**, *24*, 269.
(14) Ebdon, J. R. *Polymer* **1978**, *19*, 1233.
(15) Adachi, K.; Fujihara, I.; Ishida, Y. *J. Polym. Sci., Polym. Phys. Ed.* **1975**, *13*, 2155.
(16) Adachi, K.; Hattori, M.; Ishida, Y. *J. Polym. Sci., Polym. Phys. Ed.* **1977**, *15*, 693.
(17) Adachi, K.; Ishida, Y. *Polym. J.* **1979**, *11*, 233.
(18) Adachi, K.; Kotaka, T. *Polym. J.* **1981**, *13*, 687.
(19) Scott, R. L.; Carter, W. C.; Magat, M. *J. Am. Chem. Soc.* **1949**, *71*, 220.
(20) Minkin, V. I.; Osipov, O. A.; Zhdanov, Yu, A. "Dipole Moments in Organic Chemistry"; Hazzard, B. J., Translator; Plenum Press: New York, 1970.
(21) It was argued previously[2] that μ_1 should be a projection of the dipole vector to a line connecting C_4 and $C_{1'}$. To calculate μ_1 in this way, it is required to know the statistical weight for the internal rotation around the C_1–$C_{1'}$ bond. For the sake of simplicity, we assumed that μ_1 and μ_2 are given approximately as shown in Figure 3.
(22) Zimm, B. H.; Roe, G. R.; Epstein, L. F. *J. Chem. Phys.* **1956**, *24*, 279.
(23) "Polymer Handbook", 2nd ed.; Brandrup, J., Immergut, E. H., Eds.; Wiley: New York, 1975.

Ionic Permselectivity of Perfluorinated Ionomer Membranes

RADI AL-JISHI, VANDANA K. DATYE, and PHILIP L. TAYLOR*

Department of Physics, Case Western Reserve University, Cleveland, Ohio 44106

A. J. HOPFINGER†

Department of Macromolecular Science, Case Western Reserve University, Cleveland, Ohio 44106.

Received May 1, 1984

Ionomer membranes, with ionizable groups attached to organic polymer backbones, exhibit a large difference in permeability between oppositely charged ionic species. This permselectivity is believed to result from the electrostatic interactions at the ion exchange sites. There is mounting evidence that the ion exchange sites in these membranes phase separate from the fluorocarbon matrix to form clusters.[1-4]

The permselectivity phenomenon is made use of in separation processes where Nafion perfluorinated membranes are used in the operation of chlor-alkali cells. The current efficiency in such cells is a measure of the degree of membrane ionic selectivity. For some Nafion membranes, it has been found[5,6] that the current efficiency, when plotted against the NaOH concentration in the cathode compartment of the chlor-alkali cells, exhibits a minimum as well as a maximum, as shown schematically in Figure 1.

†Alternative address: Department of Medicinal Chemistry, Searle Research and Development, Skokie, IL 60077.

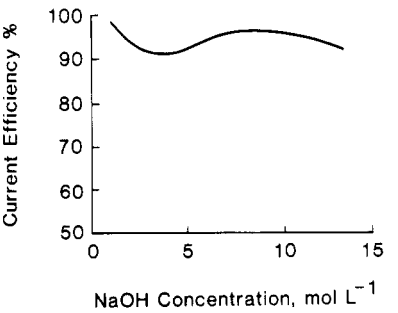

Figure 1. Schematic representation of the current efficiency as a function of NaOH catholyte concentration for Nafion membrane in a chlor-alkali cell.

Recently, Datye et al.[7] have proposed a model to explain the ionic permselectivity of Nafion membranes. In this model, it was argued that there exist dipole layers at the surface of spherical ionic clusters. The transport of ions through membranes was assumed to take place via hopping between clusters. The dipole layer at the cluster surface creates a deeper potential well for a negatively charged ion than for a positive one, thus making cation transport easier because of the lower potential barrier these ions have to overcome in order to diffuse through the membrane.

In this report we show that an extension of that model to include the dependence of the potential barrier on the water content of the membrane can account for the dependence of the current efficiency on NaOH concentration.

It is generally believed[8] that as water diffuses into the membrane, hydration shells will be formed around the negative and positive ions in the membrane clusters. We assume that oppositely charged ions exist in two possible states, either associated or dissociated. This assumption is derived from the model of Mauritz and Hopfinger[8] for the hydration-mediated dissociation equilibrium between unbound and side-chain-associated counterions in Nafion membranes. The fraction α of ion pairs remaining bound to each other will vary with the number n of water molecules present per ion pair.

In the model we consider, the dielectric constant κ will vary linearly with n for small n and will saturate at some value $1 + \kappa_0$ for infinite dilution. To fit these conditions we choose the otherwise arbitrary form

$$\kappa = 1 + \kappa_0 \tanh (n/n_0) \tag{1}$$

since the precise variation of κ with n is not important in determining the qualitative results of the model. Mauritz and Hopfinger[8] have suggested a similar but piecewise linear variant of this.

The dependence of α on n may be found by arguing that its rate of change, $d\alpha/dn$, will be governed by two factors. First, there will be a term proportional to $-\alpha$, since the number of ion pairs dissociating when $n \rightarrow n + dn$ will be proportional to the number α of bound ion pairs available. Secondly, there will also be a factor of $1 - \alpha$, since the potential barrier to release of a counterion is reduced by the number of already dissociated ions in its immediate vicinity. We thus have

$$d\alpha/dn = -c\alpha(1 - \alpha)$$

with c some constant. This has the solution

$$\alpha(n) = [1 + \exp(c(n - n_1))]^{-1} \tag{2}$$

which is the familiar Fermi–Dirac function. The constant of integration, n_1, like n_0 in eq 1, is expected to be of the order of the hydration number. In the Mauritz–Hopfinger model[8] a similar but piecewise linear form is postulated for $\alpha(n)$.

0024-9297/85/2218-0297$01.50/0 © 1985 American Chemical Society